# Radioimmunotherapy Targeting Delta-like Ligand 3 in Small Cell Lung Cancer Exhibits Antitumor Efficacy with Low Toxicity

Kathryn M. Tully[1,2,3], Salomon Tendler[2,4], Lukas M. Carter[2], Sai Kiran Sharma[2], Zachary V. Samuels[2], Komal Mandleywala[2], Joshua A. Korsen[1,2,3], Avelyn Mae Delos Reyes[1], Alessandra Piersigilli[5], William D. Travis[6], Triparna Sen[4], Nagavarakishore Pillarsetty[2], John T. Poirier[7], Charles M. Rudin[1,3,4], and Jason S. Lewis[1,2,3]

## ABSTRACT

**Purpose:** Small cell lung cancer (SCLC) is an exceptionally lethal form of lung cancer with limited treatment options. Delta-like ligand 3 (DLL3) is an attractive therapeutic target as surface expression is almost exclusive to tumor cells.

**Experimental Design:** We radiolabeled the anti-DLL3 mAb SC16 with the therapeutic radioisotope, Lutetium-177. [$^{177}$Lu]Lu-DTPA-CHX-A"-SC16 binds to DLL3 on SCLC cells and delivers targeted radiotherapy while minimizing radiation to healthy tissue.

**Results:** [$^{177}$Lu]Lu-DTPA-CHX-A"-SC16 demonstrated high tumor uptake with DLL3-target specificity in tumor xenografts. Dosimetry analyses of biodistribution studies suggested that the blood and liver were most at risk for toxicity from treatment with high doses of [$^{177}$Lu]Lu-DTPA-CHX-A"-SC16. In the radioresistant NCI-H82 model, survival studies showed that 500 μCi and 750 μCi doses of [$^{177}$Lu]Lu-DTPA-CHX-A"-SC16 led to prolonged survival over controls, and 3 of the 8 mice that received high doses of [$^{177}$Lu]Lu-DTPA-CHX-A"-SC16 had pathologically confirmed complete responses (CR). In the patient-derived xenograft model Lu149, all doses of [$^{177}$Lu]Lu-DTPA-CHX-A"-SC16 markedly prolonged survival. At the 250 μCi and 500 μCi doses, 5 of 10 and 7 of 9 mice demonstrated pathologically confirmed CRs, respectively. Four of 10 mice that received 750 μCi of [$^{177}$Lu]Lu-DTPA-CHX-A"-SC16 demonstrated petechiae severe enough to warrant euthanasia, but the remaining 6 mice demonstrated pathologically confirmed CRs. IHC on residual tissues from partial responses confirmed retained DLL3 expression. Hematologic toxicity was dose-dependent and transient, with full recovery within 4 weeks. Hepatotoxicity was not observed.

**Conclusions:** Together, the compelling antitumor efficacy, pathologic CRs, and mild and transient toxicity profile demonstrate strong potential for clinical translation of [$^{177}$Lu]Lu-DTPA-CHX-A"-SC16.

## Introduction

Small cell lung cancer (SCLC) represents approximately 15% of lung cancer diagnoses and is exceptionally lethal, accounting for over 25,000 deaths annually in the United States (1–4). Median overall survival (OS) of patients with extensive-stage disease is approximately 1 year, and the 5-year survival rate is less than 5%. SCLC is difficult to treat for a variety of reasons. At initial diagnosis, 75% to 80% of patients present with extrathoracic metastases, necessitating systemic treatment (5). While patients typically respond well to first-line therapy (usually a combination of a platinum agent, etoposide, and anti-PD-L1 immune checkpoint blockade), most patients relapse within months and responses to second- and third-line treatments are infrequent and almost universally transient.

Delta-like ligand 3 (DLL3) is a cell surface protein that has emerged as a promising candidate for targeted therapy in high-grade neuroendocrine tumors, including SCLC (6). DLL3 is notable for its tumor-selective expression profile, its high prevalence in SCLC, and its pathobiological role in this disease. DLL3 expression is induced by ASCL1, a critical transcription factor in SCLC, and has been implicated in promoting clonogenic, tumorigenic, and metastatic capacity (7–10). DLL3 expression in healthy adult tissues is almost completely intracellular, primarily confined to the Golgi apparatus (11, 12). However, it is markedly upregulated in SCLC tumors and is aberrantly trafficked to the cell surface, creating an opportunity for tumor-specific targeting (6). Approximately 72% of treatment-naïve SCLC and up to 85% of treatment-refractory SCLC stain positively for DLL3 (refs. 6, 13–15). The high prevalence of DLL3 expression makes DLL3-targeted therapies widely applicable to patients with SCLC.

Three DLL3-targeted therapeutic agents have been tested clinically: (i) the antibody–drug conjugate (ADC) rovalpituzumab-tesirine (Rova-T or SC16LD6.5), (ii) the bispecific T-cell engager (BiTE) AMG 757, and (iii) the chimeric antigen receptor T cell (CAR-T) AMG

[1]Department of Pharmacology, Weill Cornell Medicine, New York, New York. [2]Department of Radiology, Memorial Sloan Kettering Cancer Center, New York, New York. [3]Molecular Pharmacology Program, Sloan Kettering Institute, Memorial Sloan Kettering Cancer Center, New York, New York. [4]Department of Medicine, Memorial Sloan Kettering Cancer Center, New York, New York. [5]Laboratory of Comparative Pathology, Memorial Sloan Kettering Cancer Center, Weill Cornell Medicine, Hospital for Special Surgery, and The Rockefeller University, New York, New York. [6]Department of Thoracic Pathology, Memorial Sloan Kettering Cancer Center, New York, New York. [7]Perlmutter Cancer Center, New York University Langone Health, New York, New York.

**Note:** Supplementary data for this article are available at Clinical Cancer Research Online (http://clincancerres.aacrjournals.org/).

**Corresponding Authors:** Jason S. Lewis, Department of Radiology, Memorial Sloan Kettering Cancer Center, 1275 York Avenue, New York, NY 10065. Phone: 646–888–3039; E-mail: lewisj2@mskcc.org; John T. Poirier, Perlmutter Cancer Center, New York University Langone Health, 160 East 34th Street, New York, NY 10016. E-mail: john.poirier@nyulangone.org; and Charles M. Rudin, rudinc@mskcc.org

Clin Cancer Res 2022;28:1391–401

**doi:** 10.1158/1078-0432.CCR-21-1533

## Translational Relevance

Small cell lung cancer (SCLC) is a particularly lethal form of lung cancer with a 5-year survival rate of less than 5%. Although SCLC is quite radiosensitive, the majority of patients have distant metastases at the time of diagnosis, making them poor candidates for traditional external beam radiotherapy. Delta-like ligand 3 (DLL3) is an attractive target for SCLC as its expression on the cellular surface is almost exclusive to malignant tissue in adults. Herein, we developed a radioimmunotherapy approach for SCLC treatment by radiolabeling the anti-DLL3 antibody SC16 with the β particle-emitting therapeutic radioisotope Lu-177. [$^{177}$Lu]Lu-DTPA-CHX-A"-SC16 demonstrated remarkable efficacy in subcutaneous xenograft mouse models of SCLC, with mild and transient heme toxicity. These findings support [$^{177}$Lu]Lu-DTPA-CHX-A"-SC16 as a candidate for rapid clinical translation for the treatment of SCLC.

119 (16). Results of the initial clinical trials of AMG 757 and AMG 119 have not yet been published; however, Rova-T has completed phase II and phase III clinical testing in patients with SCLC (17, 18). While Rova-T initially demonstrated promising anticancer activity and validated DLL3 as a therapeutic target in SCLC, its development was ultimately stopped due to toxicity concerns that precluded repetitive dosing (17–21). The anti-DLL3 mAb of Rova-T (SC16) demonstrates high affinity and specificity but has no evident therapeutic activity against DLL3-expressing preclinical models without the cytotoxic warhead (6).

SCLC is an exceptionally radiosensitive disease. Approximately 25% of patients with limited-stage disease, confined to one hemithorax and one radiation port, are cured with external beam γ radiation with concomitant radiosensitizing chemotherapy (22). Limited-stage SCLC is the only solid tumor in which prophylactic cranial irradiation is routinely deployed to treat the possibility of microscopic and undetected disease in the brain; prophylactic cranial radiation in this context improves survival (23, 24).

In contrast to limited-stage SCLC, extensive-stage (metastatic) disease is essentially never cured by chemotherapy alone. The tumor-specific expression of DLL3 provides an opportunity to focus delivery of radiation to sites of disease in patients with SCLC, regardless of disease stage. Instead of using SC16 to deliver the pyrrolobenzodiazepine warhead to tumor cells, herein we explored the potential of using $^{177}$Lu-labeled SC16 to deliver targeted radiotherapy to SCLC tumors *in vivo*. This work builds on our prior report demonstrating successful delineation of metastatic SCLC in various murine models of the disease using $^{89}$Zr-labeled SC16 (25). By substituting Zr-89 (a PET isotope) with a β-emitting radionuclide, Lu-177, we aim to specifically direct therapeutic radiation to tumor sites throughout the body while minimizing radiation exposure to healthy tissues, something that is not feasible with conventional external beam radiation. Lu-177 is particularly well suited to anticancer treatment in a disease with a predilection for widespread metastasis. Its short tissue penetration makes it an ideal candidate for ablation of micrometastases while minimizing off-target radiation (26, 27). Herein, we report the preclinical efficacy and toxicity of $^{177}$Lu-labeled SC16—[$^{177}$Lu]Lu-DTPA-CHX-A"-SC16—for treatment of human SCLC in tumor-bearing mice.

# Materials and Methods

For details regarding antibody functionalization and radiolabeling, cell-binding assays, stability studies, single-photon emission computed tomography (SPECT) imaging, biodistribution studies, and dosimetry calculations please refer to the Supplementary Information.

### *In vivo* therapy in subcutaneous xenograft models

Mice were randomized into one of eight therapy groups ($n = 8$–10 animals per group). One day after randomization, mice were injected with vehicle (0.9% sterile saline, 50 μL via intraperitoneal injection), unmodified SC16 (60 μg via intraperitoneal injection), a single dose of ADC (0.3 mg/kg SC16LD6.5 or IgGLD6.5 via intraperitoneal injection for the H82 model, 0.4 mg/kg SC16LD6.5 via tail vein injection for the Lu149 model), or increasing doses of the radioimmunoconjugate (approximately 250, 500, or 750 μCi [$^{177}$Lu]Lu-DTPA-CHX-A"-SC16 or [$^{177}$Lu]Lu-DTPA-CHX-A"-IgG, 150 μL) via tail vein. While the activity of the radioimmunoconjugate increased between groups, the antibody mass was kept at 60 μg. Tumor volumes were measured twice weekly for 100 days posttreatment in the H82 model and 70 days posttreatment in the Lu149 model, or until mice reached a set endpoint (severe petechiae, more than 20% weight loss, or tumor volume > 2,000 mm$^3$).

### Pathology of residual tissues at tumor site

Any residual tissue remaining at the site of tumor implantation was collected upon euthanasia. Tissues were fixed in 10% neutral buffered formalin and stored in 70% ethanol at 4°C for a minimum of 10 half-lives, 67 days postadministration. Tissues were then paraffin embedded, sliced, and mounted on slides. Slides were either stained with hematoxylin and eosin (H&E) or IHC was performed. Please refer to the Supplementary Information for further details regarding IHC. Stained tissue slides were analyzed by a board-certified thoracic pathologist blinded to the treatment groups (W.D. Travis).

### Toxicity studies

Mice were monitored for outward signs of toxicity, including lethargy, loss of appetite, and petechiae. Mice were weighed twice weekly to monitor weight loss, and blood samples for hematologic analysis were collected once weekly via retro-orbital blood draws. White blood cells, red blood cells, and platelets were determined using a Hemavet 950 (Drew Scientific) or an Element HT5 (Heska Corporation) and compared with both normal range estimates for female athymic mice in the literature and baseline values that were measured prior to administration of the radiotherapeutic.

Hepatotoxicity was assessed by terminal serum hepatic enzyme levels and histologic appearance. Blood was collected at euthanasia and allowed to clot at room temperature for more than 30 minutes, then centrifuged at 2,000 g for 10 minutes. The supernatant (serum) was collected and frozen at −20°C for a minimum of 10 half-lives, 67 days. The serum alanine transaminase (ALT), aspartate transaminase (AST), and bilirubin levels were measured by the Memorial Sloan Kettering Anti-Tumor Assessment Core (New York, NY) using a Heska DC7000 Dri-chem analyzer (Heska Corporation). Livers were collected and fixed in 10% neutral buffered formalin (Thermo Fisher Scientific) for 48 hours and transferred to 70% ethanol for storage until they were processed, paraffin embedded, sliced, and mounted on slides. Sections of livers stained with H&E were analyzed for toxicity by a board-certified veterinary pathologist blinded to the treatment groups (A. Piersigilli).

### Statistical analyses

All data are shown as mean values ± SD (unless otherwise noted) and sample sizes are detailed in figure legends. Statistical analyses were performed using GraphPad Prism version 8.3.1. A $P$ value < 0.05 was considered significant. The Bonferroni correction for multiple hypothesis testing was applied where appropriate in order to minimize false-positive reporting.

### Data availability

All data generated during this study are included in this published article and its Supplementary Information files. Original data is available upon request from the corresponding authors.

## Results

### [$^{177}$Lu]Lu-DTPA-CHX-A"-SC16 demonstrates favorable biodistribution in mouse models of SCLC

To assess the potential of using SC16 as the targeting vector for radioimmunotherapy, unmodified SC16 antibody was bioconjugated to *p*-SCN-Bn-CHX-A"-DTPA and radiolabeled with Lu-177 (**Fig. 1A**). The chelate *p*-SCN-Bn-CHX-A"-DTPA was chosen instead of a dodecane tetraacetic acid (DOTA) analogue to avoid the high temperature otherwise required for radiolabeling, which could disrupt antibody stability. After bioconjugation of the *p*-SCN-Bn-CHX-A"-DTPA to SC16, the immunoconjugates were analyzed using matrix-assisted laser desorption/ionization–time-of-flight (MALDI-TOF) MS/MS. The calculated average number of DTPA chelates per SC16 antibody was 1.4 ± 0.1 (Supplementary Fig. S1). Radiolabeling the SC16-CHX-A"-DTPA conjugates yielded high radiochemical yield (≥95%) and specific activity (13–18 mCi/mg), an outcome indicative of favorable bioconjugation (Supplementary Fig. S2A). [$^{177}$Lu]Lu-DTPA-CHX-A"-SC16 radioimmunoconjugate was isolated with high radiochemical purity (≥ 99%) and demonstrated ≥ 95% serum stability when incubated in human serum at 37°C for 7 days (Supplementary Figs. S2B and S3).

Having confirmed reproducible production of high specific activity [$^{177}$Lu]Lu-DTPA-CHX-A"-SC16, we sought to confirm the immunoreactivity of the radioimmunoconjugate using the same cell lines that would be used for *in vivo* studies. The SCLC NCI-H82 line was selected as a DLL3-positive line and A549 cells were used as a negative control. Previous studies by our group have shown that H82 cells have median DLL3 expression among a cohort of SCLC lines, and we had successfully imaged H82 xenograft tumors *in vivo* using $^{89}$Zr-labeled SC16 (25). H82 was derived from the pleural fluid of a patient with recurrent and progressive disease after prior chemotherapy and chest radiotherapy, a similar context in which radioimmunotherapy might be applied clinically (28). Furthermore, H82 xenografts demonstrate rapid growth in athymic nude mice and are notably radioresistant, setting a high bar for *in vivo* efficacy (29).

To confirm the immunoreactivity of the SC16 antibody for DLL3 postbioconjugation and radiolabeling, cell-binding assays were performed using H82 and A549 cells. [$^{177}$Lu]Lu-DTPA-CHX-A"-SC16 demonstrated approximately 40-fold differential binding favoring H82, with some (1.2%) nonspecific uptake in A549 cells (**Fig. 1B**). To assess maintenance and homogeneity of DLL3 expression, H82 and A549 cells were subcutaneously xenografted into athymic nude mice and allowed to grow to a volume of 2,000 mm$^3$, and sections of formalin-fixed, paraffin-embedded (FFPE) tumors were stained for DLL3 expression. DLL3 IHC confirmed strong staining in the H82 tumors and minimal staining in the A549 tumors (**Fig. 1C**). Notably, H82 tumors showed membrane-localized staining that colocalized with the viable SCLC cells seen in the H&E and Ki67 IHC (Supplementary Fig. S4).

*Ex vivo* biodistribution profiles of the SC16 versus isotype control radioimmunoconjugates were assessed in non–tumor-bearing mice as well as mice bearing subcutaneous H82 and A549 xenografts by injection of either [$^{177}$Lu]Lu-DTPA-CHX-A"-SC16 or[$^{177}$Lu]Lu-DTPA-CHX-A"-IgG (10–30 μCi; 3 μg in 150 μL PBS; $n = 3$). Organ uptake was quantified by dividing the decay-corrected percent of the injected dose (%ID) per tissue mass. In non–tumor-bearing mice, organ uptake of [$^{177}$Lu]Lu-DTPA-CHX-A"-SC16 decreased over time, with the highest radioactivity concentrations in the blood and liver (10.1 ± 2.2 and 12.5 ± 1.9% ID/g at 120 hours, respectively; Supplementary Fig. S5A). The biodistribution of [$^{177}$Lu]Lu-DTPA-CHX-A"-IgG in non–tumor-bearing mice followed similar trends but had lower uptake in the liver and spleen (Supplementary Fig. S5B). To evaluate nonspecific tumor uptake, the biodistribution of [$^{177}$Lu]Lu-DTPA-CHX-A"-SC16 and [$^{177}$Lu]Lu-DTPA-CHX-A"-IgG was profiled in mice bearing DLL3-negative A549 subcutaneous xenografts. The biodistribution profiles were consistent with those observed in non–tumor-bearing mice, and nonspecific uptake in the tumor only reached 4.2 ± 0.9 and 6.4 ± 1.9% ID/g for [$^{177}$Lu]Lu-DTPA-CHX-A"-SC16 and [$^{177}$Lu]Lu-DTPA-CHX-A"-IgG, respectively (Supplementary Fig. S6A and S6B). Finally, the biodistribution profiles were compared in mice bearing DLL3-positive H82 subcutaneous xenografts. [$^{177}$Lu]Lu-DTPA-CHX-A"-SC16 showed high tumor uptake in mice bearing H82 subcutaneous xenografts, with uptake reaching 95 ± 14% ID/g at 120 hours postinjection (p.i.; **Fig. 1D**; see Supplementary Fig. S7A for full biodistribution data). Specificity of uptake was demonstrated by codosing [$^{177}$Lu]Lu-DTPA-CHX-A"-SC16 with a 100-fold excess of unlabeled SC16 antibody and euthanizing the mice at 72 hours p.i. to evaluate blockade of DLL3-mediated accretion of radioactivity in the tumor. Qualitative SPECT images of mice bearing H82 tumors confirmed the *ex vivo* biodistribution data showing high tumor uptake and minimal uptake in nontarget organs (**Fig. 1E**). The focal enrichment of [$^{177}$Lu]Lu-DTPA-CHX-A"-SC16 outside of the tumor that is seen in the maximum intensity projection (MIP) is nonspecific lymph node uptake; this is also seen in the MIPs when performing immunoPET imaging using the [$^{89}$Zr]Zr-DFO-SC16 construct, and it is consistent across various subcutaneous xenograft models in athymic mice. Notably, this nonspecific lymph node uptake is not seen when using [$^{89}$Zr]Zr-DFO-SC16 to image DLL3 expression in human patients with SCLC (NCT04199741), and thus should not pose a risk for radioimmunotherapy. The *ex vivo* biodistribution of isotype control [$^{177}$Lu]Lu-DTPA-CHX-A"-IgG in mice bearing H82 xenografts was also assessed, and nonspecific tumor uptake peaked at 7.5 ± 1.6% ID/g at 72 hours p.i. (Supplementary Fig. S7B).

### Mouse dosimetry indicates blood and liver are the highest concerns for toxicity

Dosimetry calculations were performed prior to radiotherapy experiments to guide dose selection and determine which organs would be most at risk for toxicity from radiation exposure. To generate conservative estimates, dosimetry estimates for nontarget organs were calculated using biodistribution data from non–tumor-bearing mice. Because exogenous macromolecules such as antibodies are catabolized *in vivo* via the reticuloendothelial system, it was unsurprising that the liver had the highest calculated absorbed dose among nontarget organs (**Table 1**). Notably, the liver can tolerate relatively high radiation exposure (approximately 30 Gy), so hepatotoxicity would not be expected in animals receiving lower doses of radiolabeled antibody. Based on dosimetry calculations and the differential radiosensitivity of

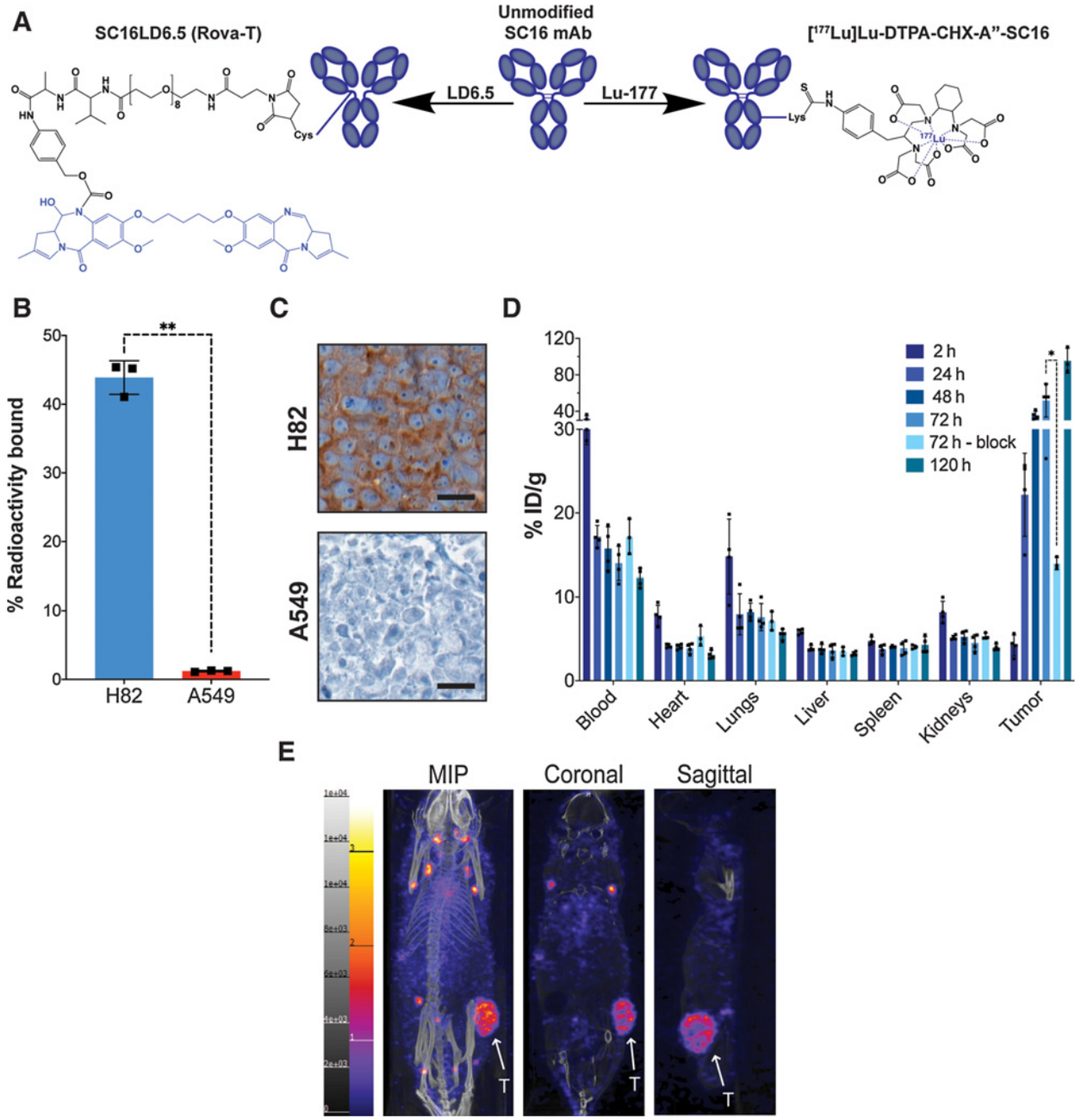


**Figure 1.**

**A,** Representative structures of the unmodified SC16 antibody, the ADC SC16LD6.5 (Rov-T), and the radioimmunoconjugate [$^{177}$Lu]Lu-DTPA-CHX-A"-SC16. The cytotoxic moieties of each therapeutic are highlighted in blue. **B,** A radioligand binding assay of [$^{177}$Lu]Lu-DTPA-CHX-A"-SC16 in H82 and A549 cells. Error bars represent SD ($n = 3$). An unpaired, two-tailed *t* test was performed ($P = 0.001$). **C,** DLL3 IHC on subcutaneous tumor xenografts. Scale bar: 20 μm. See Supplementary Fig. S4. Mouse 108 for the lower magnification image of the H82 tumor DLL3 IHC and corresponding histology. **D,** The *ex vivo* biodistribution data of select organs from athymic mice bearing subcutaneous H82 xenografts after the administration of [$^{177}$Lu]Lu-DTPA-CHX-A"-SC16 (10–30 μCi; 3 μg in 150 μL PBS; $n = 3$ mice per time point) via tail vein. The tumor uptake at 72 hours was sufficiently blocked using 100-fold excess of unlabeled SC16 ($P = 0.0212$). See Supplementary Fig. S9 for the uptake in all organs collected. **E,** Representative whole-body SPECT/CT images of athymic mice bearing subcutaneous H82 xenografts 120 hours after the administration of [$^{177}$Lu]Lu-DTPA-CHX-A"-SC16 (1,050–1,100 μCi; 60–70 μg in 150 μL PBS) via tail vein. The tumors (indicated by white arrows) can clearly be delineated in the MIP, coronal, and sagittal images. h, hours.

**Table 1.** Mouse and human dosimetry of [$^{177}$Lu]Lu-DTPA-CHX-A"-SC16.

| Organ | Mouse | | Human |
|---|---|---|---|
| | Absorbed dose coefficient (Gy/mCi) | Therapeutic index | Absorbed dose coefficient (mGy/mCi) |
| Red marrow | 16.7 | 23.0 | 10.5 |
| Lungs | 34.1 | 11.2 | 4.03 |
| Liver | 91.9 | 4.2 | 84.7 |
| Spleen | 51.1 | 7.5 | 27.1 |
| Kidneys | 28.2 | 13.6 | 25.7 |
| Total body | 31.0 | 12.4 | 10.7 |
| Tumor | 383.3 | — | — |

Note: The absorbed doses for nontarget organs were calculated using the biodistribution data in non–tumor-bearing athymic mice. The absorbed tumor dose was calculated using the biodistribution data in athymic female mice bearing subcutaneous H82 xenografts.

nontarget organs, we chose to dose animals with 250, 500, and 750 μCi of radiolabeled antibody.

### [$^{177}$Lu]Lu-DTPA-CHX-A"-SC16 demonstrates robust efficacy in mouse models of SCLC

To assess the therapeutic potential of $^{177}$Lu-labeled SC16, we randomized mice bearing subcutaneous H82 xenografts into eight groups ($n = 8$–10 mice per group). Animals were given vehicle (0.9% sterile saline, 50 μL via intraperitoneal injection), a single dose of ADC (either 0.3 mg/kg SC16LD6.5 or IgGLD6.5 via intraperitoneal injection), unmodified SC16 (60 μg, 150 μL via tail vein injection), or radioimmunoconjugate. The radioimmunoconjugate cohorts were 750 μCi of [$^{177}$Lu]Lu-DTPA-CHX-A"-IgG control (60 μg, 150 μL via tail vein) or increasing doses of the targeting SC16 radioimmunoconjugate (approximately 250, 500, or 750 μCi of [$^{177}$Lu]Lu-DTPA-CHX-A"-SC16; 60–70 μg, 150 μL via tail vein injection). As anticipated, the tumors in the saline, IgGLD6.5, and unmodified SC16 control cohorts all progressed to 2,000 mm$^3$ at similar rates, indicating these treatments had no efficacy (**Fig. 2A**; Supplementary Figs. S8–S10). All mice in the [$^{177}$Lu]Lu-DTPA-CHX-A"-IgG group developed severe petechiae within the first 10 days, and all mice had to be euthanized by 13 days posttreatment (**Fig. 2A–C**; Supplementary Fig. S11). Surprisingly, the tumors in the SC16LD6.5 cohort demonstrated only a minor and statistically insignificant decrease in tumor progression and no significant improvement in survival relative to the saline control cohort (**Fig. 2A–C**; Supplementary Fig. S12). MALDI-TOF MS/MS was performed to confirm that the SC16LD6.5 was pure and intact (Supplementary Fig. S13). An *in vitro* cytotoxicity assay was also performed and the $EC_{50}$ of SC16LD6.5 in H82 cells was determined to be 3.7 pmol/L (Supplementary Fig. S14). The low picometer *in vitro* $EC_{50}$ confirmed that the SC16LD6.5 was intact and functional; the lack of *in vivo* efficacy could have been a consequence of suboptimal dosing, although this dosing regimen had demonstrated efficacy in other preclinical models (30, 31).

The [$^{177}$Lu]Lu-DTPA-CHX-A"-SC16 radiotherapy demonstrated progressive dose-dependent efficacy. Tumors in the lowest activity cohort (250 μCi) reached 2,000 mm$^3$ at a rate indistinguishable from SC16LD6.5 and did not show improved survival over saline control (**Fig. 2A–C**; Supplementary Fig. S15). Tumors in animals assigned to the medium and high activity cohorts (500 and 750 μCi, respectively) both demonstrated tumor reduction approximately 7 to 13 days posttreatment consistent with antitumor efficacy (**Fig. 2A**). Within the 500 μCi cohort, some animals experienced deep but transient partial responses (PR; e.g., mouse 122, Supplementary Fig. S16) while others demonstrated responses that were sustained for the entire 100 days of the study (e.g., mouse 117; Supplementary Fig. S16). The median survival for the 500 μCi cohort was 80 days posttreatment, significantly higher than the saline treatment group (**Fig. 2B** and **C**; $P = 0.0003$). At 100 days posttreatment, 2 of the 8 mice in the 500 μCi dose cohort had not reached an endpoint.

The [$^{177}$Lu]Lu-DTPA-CHX-A"-SC16 cohort that received 750 μCi [$^{177}$Lu]Lu-DTPA-CHX-A"-SC16 demonstrated deeper and more durable antitumor responses (**Fig. 2A**; Supplementary Fig. S17). OS in this cohort was significantly longer than the saline control, with the median survival not determined as 6 of the 8 mice had not reached a defined endpoint by 100 days posttreatment (**Fig. 2B** and **C**; Supplementary Fig. S17; $P < 0.0001$). Of these 6 mice, 3 had evident residual tumor at the site of implantation, while the other 3 had no palpable residual tumor.

Because of the impressive efficacy demonstrated in the radioresistant H82 model and to assess the broader applicability of the radioconjugate, we repeated the therapy experiments in a subcutaneous patient-derived xenograft model to confirm our findings. The PDX Lu149 was selected for its medium DLL3 expression and ability to grow in athymic nude mice (25). Biodistribution studies were performed to confirm tumor uptake and favorable tumor-to-tissue uptake ratios. Tumor uptake of [$^{177}$Lu]Lu-DTPA-CHX-A"-SC16 was lower in the Lu149 xenografts, but still reached 74 ± 7% ID/g at 120 hours p.i. (Supplementary Fig. S19). The blood uptake of the radioconjugate was slightly higher in the Lu149 model than in the H82 model (Supplementary Fig. S20). Cohorts of tumor-bearing mice were treated with vehicle (0.9% sterile saline, 50 μL), a single dose of 0.4 mg/kg SC16LD6.5, or radioimmunoconjugate via tail vein injections ($n =$ 9–10 per group). The radioimmunoconjugate cohorts for the Lu149 therapy studies were the same used in the H82 studies; 750 μCi of [$^{177}$Lu]Lu-DTPA-CHX-A"-IgG control (60 μg, 150 μL via tail vein) or increasing doses of the targeting SC16 radioimmunoconjugate (approximately 250, 500, or 750 μCi of [$^{177}$Lu]Lu-DTPA-CHX-A"-SC16; 60–70 μg, 150 μL via tail vein injection). Prior publications and our H82 therapy data confirmed that neither unmodified SC16 or IgGLD6.5 demonstrated antitumor efficacy, so these two cohorts were not included in the Lu149 therapy studies.

Tumors in the saline-treated cohort rapidly grew to 2,000 mm$^3$, resulting in a median survival of 23 days (**Fig. 2D–F**; Supplementary Fig. S21). Consistent with a prior report (6), SC16LD6.5 demonstrated efficacy in the Lu149 model, with slowed tumor progression and improved survival over the saline cohort (median survival 54 days; **Fig. 2D–F**; Supplementary Fig. S22; $P < 0.0001$). In contrast with the H82 studies, not all mice treated with 750 μCi [$^{177}$Lu]Lu-DTPA-CHX-A"-IgG developed severe petechiae; 3 of the 9 mice developed petechiae severe enough to warrant euthanasia, but the remaining 6 mice demonstrated no or very mild petechiae. For the mice that did not demonstrate severe petechiae, treatment with 750 μCi [$^{177}$Lu]Lu-DTPA-CHX-A"-IgG led to delayed tumor growth curve, and an overall improved median survival of 47 days (**Fig. 2D–F**; Supplementary Fig. S23; $P = 0.0193$).

The [$^{177}$Lu]Lu-DTPA-CHX-A"-SC16 radiotherapy demonstrated impressive antitumor efficacy in the Lu149 model, even at low and moderate doses. Nine of the 10 tumors in the lowest activity cohort (250 μCi) demonstrated complete responses (CR), defined as the tumor volume remaining less than 100 mm$^3$ (to account for residual scar tissue at the implantation site) 70 days p.i. (**Fig. 2D**;

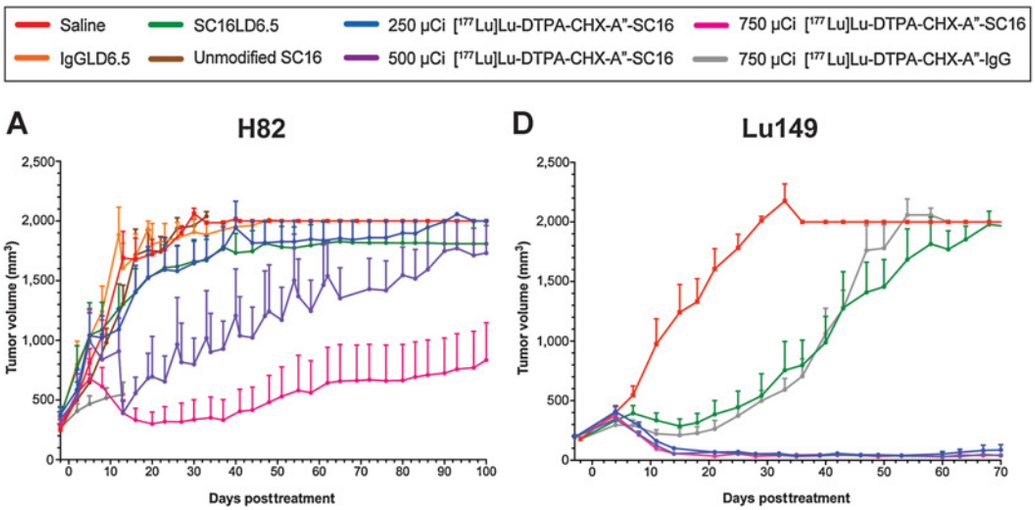


C

| Treatment | Median survival (days) |
|---|---|
| Saline | 16 |
| SC16LD6.5 | 21 |
| 250 μCi [$^{177}$Lu]Lu-DTPA-CHX-A"-SC16 | 23 |
| 500 μCi [$^{177}$Lu]Lu-DTPA-CHX-A"-SC16 | 79.5*** |
| 750 μCi [$^{177}$Lu]Lu-DTPA-CHX-A"-SC16 | und**** |
| 750 μCi [$^{177}$Lu]Lu-DTPA-CHX-A"-IgG | 13 |
| IgGLD6.5 | 16 |
| Unmodified SC16 | 19 |

F

| Treatment | Median survival (days) |
|---|---|
| Saline | 23 |
| SC16LD6.5 | 54**** |
| 250 μCi [$^{177}$Lu]Lu-DTPA-CHX-A"-SC16 | und**** |
| 500 μCi [$^{177}$Lu]Lu-DTPA-CHX-A"-SC16 | und**** |
| 750 μCi [$^{177}$Lu]Lu-DTPA-CHX-A"-SC16 | und* |
| 750 μCi [$^{177}$Lu]Lu-DTPA-CHX-A"-IgG | 47* |

**Figure 2.**

**A,** The average tumor volume of mice bearing H82 xenografts after treatment (error bars indicate SD; $n = 8$–10). The averages were adjusted by including the final tumor volume of each mouse if the mouse reached its endpoint prior to 100 days posttreatment (e.g., if a mouse reached its endpoint on day 20, the volume of the tumor on day 20 was still included in the averages after day 20 despite the mouse being euthanized). **B,** Percent survival as a function of time for mice bearing H82 xenografts following the administration of treatment or vehicle. Log-rank tests were performed for comparing each treatment with saline cohort [shading indicates 95% confidence interval (CI); $n = 8$–10; *** $P = 0.0003$, **** $P < 0.0001$]. **C,** The median survival of mice bearing H82 xenografts posttreatment. Log-rank tests were performed for comparing each treatment to saline cohort ($n = 8$–10; *** $P = 0.0003$, **** $P < 0.0001$). **D,** The average tumor volume of mice bearing Lu149 xenografts after treatment (error bars indicate SD; $n = 9$–10). The averages were adjusted by including the final tumor volume of each mouse if the mouse reached its endpoint prior to 100 days posttreatment (e.g., if a mouse reached its endpoint on day 20, the volume of the tumor on day 20 was still included in the averages after day 20 despite the mouse being euthanized). **E,** Percent survival as a function of time for mice bearing Lu149 xenografts following the administration of treatment or vehicle. Log-rank tests were performed for comparing each treatment with saline cohort (shading indicates 95% CI; $n = 9$–10; * $P = 0.0108$ and 0.0193 for 750 μCi [$^{177}$Lu]Lu-DTPA-CHX-A"-SC16 and [$^{177}$Lu]Lu-DTPA-CHX-A"-IgG, respectively; **** $P < 0.0001$). **F,** The median survival of mice bearing Lu149 xenografts posttreatment. Log-rank tests were performed for comparing each treatment with saline cohort ($n = 9$–10; * $P = 0.0108$ and 0.0193 for 750 μCi [$^{177}$Lu]Lu-DTPA-CHX-A"-SC16 and [$^{177}$Lu]Lu-DTPA-CHX-A"-IgG, respectively; **** $P < 0.0001$). und, undefined.

Supplementary Fig. S24). One mouse had a deep and sustained PR, with the tumor only beginning to grow back 50 days p.i. (mouse 406, Supplementary Fig. S24). All mice were still alive at 70 days p.i.; median survival was not defined but was significantly longer than the saline control cohort (**Fig. 2E** and **F**; $P < 0.0001$). The tumors in the 500 μCi cohort demonstrated similar results, with all 10 mice having CRs for the duration of the study and a significantly improved survival with an undefined median (**Fig. 2D–F**; Supplementary Fig. S25; $P < 0.0001$).

The [$^{177}$Lu]Lu-DTPA-CHX-A"-SC16 cohort that received 750 μCi [$^{177}$Lu]Lu-DTPA-CHX-A"-SC16 also demonstrated deep and durable antitumor responses (**Fig. 2D**; Supplementary Fig. S26). However, 4 of the 10 mice developed severe petechiae around days 10 to 13 p.i. and were therefore euthanized. Of the 6 mice that did not develop severe enough petechiae to warrant euthanasia, all demonstrated CRs for the duration of the study. The OS again was significantly longer than the saline control, with median survival not determined as 6 of the 10 mice had not reached a defined endpoint by 70 days p.i. (**Fig. 2E** and **F**; $P = 0.01$).

### Histology on residual tissue at tumor implantation site confirms CRs and demonstrates DLL3 expression in PRs

At necropsy, tumor beds from all mice were sectioned for H&E staining and Ki67 IHC was performed to assess for residual microscopic tumor (**Fig. 3A**). In the H82-bearing mice treated with 750 μCi [$^{177}$Lu]Lu-DTPA-CHX-A"-SC16, 3 of the 6 mice still alive at 100 days did not have palpable tumors. No viable tumor was observed in any of these three animals; the sites of prior tumor growth revealed a combination of fibrosis, necrosis, calcification, and infiltrating histiocytes. In the Lu149 group, 9 of the 10 mice that were treated with 250 μCi [$^{177}$Lu]Lu-DTPA-CHX-A"-SC16 had tumors that were either not palpable or remained less than 100 mm$^3$ for over 2 months posttreatment. Of these nine tumors, five were pathologically confirmed CRs with no residual viable tumor tissue. In the Lu149-bearing mice treated with 500 μCi [$^{177}$Lu]Lu-DTPA-CHX-A"-SC16, the pathologist determined that seven of the nine tumor beds had no viable tumor, confirming CRs. Finally, in the Lu149-bearing mice that received 750 μCi [$^{177}$Lu]Lu-DTPA-CHX-A"-SC16 and did not require euthanasia for heme toxicity, all of the 6 mice had tumors that were pathologically confirmed CRs.

While the efficacy experiments were designed to assess the relative benefit of a single dose of therapeutic radioconjugate, repeated dosing should be beneficial in achieving further tumor reduction, and fractionated dosing using lower amounts of activity could ameliorate the toxicity associated with a maximal activity single dose. To determine whether repeated dosing would be feasible in mice demonstrating a PR to [$^{177}$Lu]Lu-DTPA-CHX-A"-SC16, we assessed DLL3 target expression on tumors from animals that had experienced PRs. Examination of tumors at necropsy from these animals demonstrated viable tumor that retained DLL3 expression which colocalized with areas of viability as assessed by Ki67 (**Fig. 3B** and **C**). These data support the rationale for repeat dosing of [$^{177}$Lu]Lu-DTPA-CHX-A"-SC16.

[$^{177}$Lu]Lu-DTPA-CHX-A"-SC16 demonstrates transient heme toxicity and no significant hepatotoxicity

Finally, we wanted to address the concern of the toxicity from [$^{177}$Lu]Lu-DTPA-CHX-A"-SC16 treatment, as severe toxicity would hinder its translational potential. Mice were weighed twice weekly, and none of the cohorts demonstrated significant weight loss (Supplementary Fig. S28). From dosimetry estimates, we anticipated that blood and liver would be primary concerns for toxicity. To assess heme toxicity, complete blood count analyses were performed weekly for the duration of the study. The pretreatment ranges for white blood

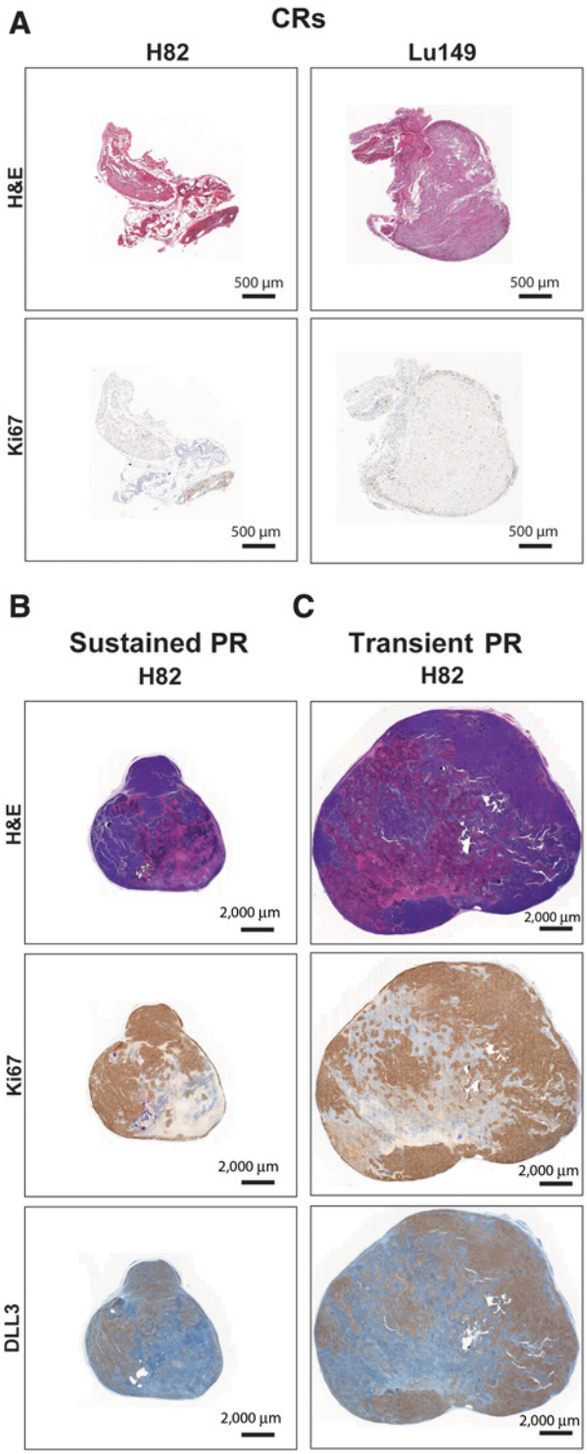


**Figure 3.**

**A,** Representative H&E staining and Ki67 IHC of residual tissues from tumor beds of mice that demonstrated CRs (H82 mouse 114 and Lu149 mouse 428). Scale bar: 500 μm. **B,** Representative H&E staining, Ki67 IHC, and DLL3 IHC of the tumor from a mouse that demonstrated a sustained PR (H82 mouse 126). Scale bar: 2,000 μm. **C,** Representative H&E staining, Ki67 IHC, and DLL3 IHC of the tumor from a mouse that demonstrated a transient PR (H82 mouse 122). Scale bar: 2,000 μm.

cells (WBC), red blood cells (RBC), and platelets were calculated as averages ± one SD (**Fig. 4A–F**; grey box). All three of these parameters demonstrated dose-dependent decreases in both the H82 and Lu149 models. In the H82-bearing mice, all cell types recovered and were consistently within the normal ranges established for female athymic mice (indicated by grey dotted lines, **Fig. 4A–C**) by 4 weeks posttreatment. Notably, none of the H82-bearing mice that received [$^{177}$Lu]Lu-DTPA-CHX-A"-SC16 exhibited petechiae, despite a transient decrease in platelet counts (**Fig. 4C**). In the Lu149-bearing mice the blood components took longer to recover, with the WBCs, RBCs, and platelets reaching healthy ranges by 8, 7, and 4 weeks, respectively (**Fig. 4D–F**). Overall, the hematologic lineages demonstrated dose-dependent and transient decreases with a nadir of 2 to 3 weeks postdose, and full recovery to the defined normal ranges.

To evaluate for possible hepatotoxicity, serum and liver were collected for analysis from each mouse bearing an H82 xenograft at euthanasia. ALT, AST, and bilirubin serum levels were measured as markers for hepatotoxicity (**Fig. 4G–I**). Relative to the saline cohort, none of these biomarkers demonstrated increased levels at any of the activity doses of [$^{177}$Lu]Lu-DTPA-CHX-A"-SC16. The spectrum of morphologic changes observed in the livers of both treated and control animals was consistent with a minimal to mild perivascular (mostly periportal) infiltration of lymphocytes, a common finding in non–specific pathogen-free (SPF) mice (Supplementary Fig. S29). Hepatocellular vacuolation and/or hypertrophy were observed rarely (1/6 in the 500 μCi cohort, 1/8 in the 750 μCi cohort) and were hence considered an incidental finding. Minimal hepatocellular degeneration was observed in 1 of the 250 μCi cohort mice, but is a frequent incidental finding even in experimentally naïve mice (32–34). No correlation was found between the AST and ALT elevation in individual mice with any of these liver changes, together indicating a lack of significant hepatotoxicity at any of the [$^{177}$Lu]Lu-DTPA-CHX-A"-SC16 doses assessed in the H82-bearing mice.

Serum was also collected at euthanasia from mice bearing Lu149 xenografts, and hepatic enzyme levels were determined to confirm that hepatotoxicity remained negligible. Relative to the saline cohort, AST was the only biomarker that demonstrated significantly increased levels at the 250 and 500 μCi dose cohorts, and none of the biomarkers demonstrated significantly increased levels in the mice treated with 750 μCi [$^{177}$Lu]Lu-DTPA-CHX-A"-SC16 (**Fig. 4J–L**; $P = 0.0044$ and 0.0067 for 250 and 500 μCi [$^{177}$Lu]Lu-DTPA-CHX-A"-SC16, respectively). Because a significant increase was only observed in one of the three biomarkers, and an increase was not observed in the highest activity cohort, we concluded that hepatoxicity remained insignificant in the Lu149 xenograft model.

## Discussion

The paucity of clinical advances in the treatment of SCLC combined with the exceptionally high mortality rate have led the NCI to designate SCLC as one of only two diseases prioritized under the U.S. Recalcitrant Cancer Research Act (35). Clearly, there is an unmet clinical need to develop novel and more durable effective therapeutic approaches for the treatment of SCLC. The nearly universal inactivation or deletion of genes encoding the key cell cycle regulators TP53 and RB1 promotes the rapid and uncontrolled proliferation of this cancer. However, these transformational changes also make it uniquely vulnerable: this tumor is highly sensitive to single and double strand DNA breaks, such as those induced by high energy radiation. While highly effective within the treatment field, a substantial practical limitation of external beam radiation is the inability to address the widespread overt and subclinical metastatic deposits that characterize SCLC. Systemic radioimmunotherapy employing a mAb with high specificity for DLL3, a target selectively expressed on the tumor cell surface, can overcome this limitation by delivering targeted radiation to sites of disease. Here we explored this strategy in a proof-of-principle study in tumor-bearing mice, demonstrating remarkable efficacy *in vivo*.

[$^{177}$Lu]Lu-DTPA-CHX-A"-SC16 administered at 500 or 750 μCi doses had substantially higher and more durable antitumor efficacy than the previously clinically active ADC SC16LD6.5 (Rova-T) in H82 xenografts, with minimal and transient hemetoxicity. Although the SC16LD6.5 dose regimen we selected demonstrated efficacy in other preclinical models, suboptimal dosing could have caused the lack of efficacy shown. Another possible explanation for limited *in vivo* efficacy of SC16LD6.5 in this xenograft model could be a shared resistance mechanism between the pyrrolobenzodiazepine (PBD) warhead and prior lines of treatment, which for the patient H82 was derived from included high-dose cyclophosphamide, methotrexate, and 1-(2-chloroethyl)-3-cyclohexyl-l-nitrosourea (CCNU) followed by vincristine, adriamycin, and procarbazine (28).

In Lu149 xenografts, [$^{177}$Lu]Lu-DTPA-CHX-A"-SC16 administered at 250, 500, or 750 μCi doses demonstrated even more impressive antitumor efficacy, with concerning heme toxicity only at the highest activity dose. We believe the observed variation in toxicity between the H82 and Lu149 xenografts is attributable to the difference in tumor uptake. Because the average tumor uptake in the Lu149 xenografts is almost 20% ID/g lower than uptake in the H82 tumors at 120 hours p.i., more radioconjugate remains in the blood in the Lu149 model, and this increase in activity in the blood may result in greater heme toxicity. This hypothesis is also supported by the severe petechiae seen in the mice who received the nontargeting [$^{177}$Lu]Lu-DTPA-CHX-A"-IgG as the nontargeting radioconjugate only has minimal nonspecific intratumoral accumulation.

Despite the heme toxicity seen in some Lu149-bearing mice that received 750 μCi [$^{177}$Lu]Lu-DTPA-CHX-A"-SC16, single doses at 250 or 500 μCi still led to pathologically confirmed CRs, indicating that higher activity doses might be unnecessary in more radiosensitive tumors. While both tumor models display aggressive growth *in vivo*, the radiotherapeutic displayed more impressive antitumor efficacy in the Lu149 xenografts than the H82 xenografts because we specifically chose the H82 xenografts for their radioresistance. As previously discussed, the H82 cell line was derived from a patient that had been heavily pretreated and was highly resistant to DNA-damaging agents, while the Lu149 xenograft model was derived from a patient that was treatment naïve. Therefore even though the Lu149 xenografts display lower DLL3 expression than the H82 xenografts (and therefore lower tumor uptake of the radiotherapeutic), the intrinsic sensitivity of each tumor to DNA damage is vastly different, leading to the difference in therapeutic response. Nevertheless, the Lu149 PDX may represent more typical radiosensitivity of SCLC and offers strong evidence for the clinical potential of [$^{177}$Lu]Lu-DTPA-CHX-A"-SC16.

While it was particularly striking that multiple H82-bearing mice and the majority of Lu149-bearing mice had pathologically confirmed CRs, CR to a single dose of the radioconjugate is unlikely in patients with bulkier disease. The initial toxicity profile of [$^{177}$Lu]Lu-DTPA-CHX-A"-SC16 and retention of DLL3 expression after initial dosing suggests that this agent could be periodically administered in cycles allowing for hematologic recovery. Multiple $^{177}$Lu-antibody conjugates have been tested in clinical trials, and their heme toxicity in human patients is well established and manageable, in contrast to SC16LD6.5 for which adverse effects related to the PBD warhead precluded repetitive dosing in patients (19–21).

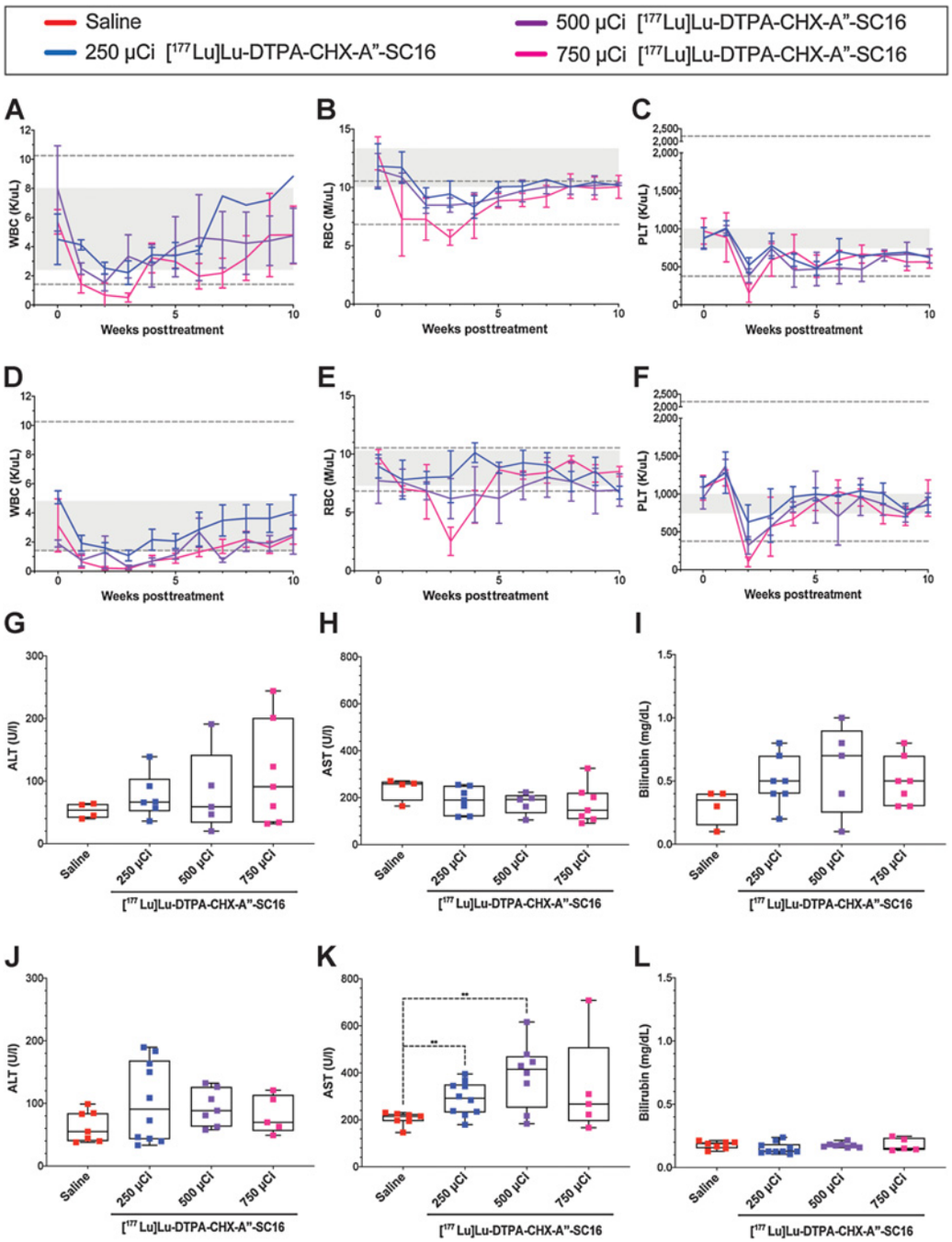


**Figure 4.**

**A–C,** WBC counts, RBC counts, and platelet counts of micebearing H82 xenografts who received [$^{177}$Lu]Lu-DTPA-CHX-A"-SC16. Complete blood count analyses were performed once a week on a subset of the animals used in the survival study ($n = 3$–4). Twenty parameters were recorded, and three are represented. Values are represented as means with error bars indicating SD. Grey boxes indicate the mean ± SD of values collected from the entire cohort of H82-bearing mice 2 days prior to therapy administration. Grey dotted lines indicate the healthy range for female athymic mice. **D–F,** WBC counts, RBC counts, and platelet counts of mice bearing Lu149 xenografts who received [$^{177}$Lu]Lu-DTPA-CHX-A"-SC16. Complete blood count analyses were performed once a week on a subset of the animals used in the survival study ($n = 3$–4). Twenty parameters were recorded, and three are represented. Values are represented as means with error bars indicating SD. Grey boxes indicate the mean ± SD of values collected from the entire cohort of Lu149-bearing mice 2 days prior to therapy administration. Grey dotted lines indicate the healthy range for female athymic mice. **G–I,** Box plots of the terminal ALT, AST, and bilirubin serum levels from H82-bearing mice used in the survival study. Multiple *t* tests were performed comparing each radiotherapy cohort with saline, and no significant differences were found ($n = 4$–7). **J–L,** Box plots of the terminal ALT, AST, and bilirubin serum levels from Lu149-bearing mice used in the survival study. Multiple *t* tests were performed comparing each radiotherapy cohort with saline ($n = 5$–10; ** $P = 0.0044$ and 0.0067 for 250 and 500 μCi [$^{177}$Lu]Lu-DTPA-CHX-A"-SC16, respectively).

The demonstrated efficacy of [$^{177}$Lu]Lu-DTPA-CHX-A"-SC16 can be considered in context of our previously published studies demonstrating that the SC16 antibody can be repurposed for robust immunoPET imaging of SCLC using $^{89}$Zr ([$^{89}$Zr]Zr-DFO-SC16) (25). $^{89}$Zr-immunoPET of patients with SCLC to identify those who would benefit from targeted radioimmunotherapy with [$^{177}$Lu]Lu-DTPA-CHX-A"-SC16 would appear to be a clinically viable approach. An analogous approach is currently being tested clinically using the 5B1 antibody in pancreatic ductal adenocarcinoma (NCT02687230 and NCT03118349). The trace doses of [$^{89}$Zr]Zr-DFO-SC16 used for PET imaging would not preclude uptake of the therapeutic radioimmunoconjugate. ImmunoPET of patients with SCLC with [$^{89}$Zr]Zr-DFO-SC16 is currently underway (NCT04199741).

The promising efficacy demonstrated here, with multiple pathologically confirmed CRs and minimal evident toxicity at effective activity doses, contrasts with a recent report by Lakes and colleagues exploring anti-DLL3 radioimmunotherapy using both Lu-177 and the alpha emitter Ac-225 (36). The Lakes study employed NOD/SCID mice and demonstrated dose-limiting hematologic toxicity in the range of 21 to 64 μCi with a $^{177}$Lu-labeled antibody, which is below the effective range defined in our analysis of H82 and Lu149 xenografts. We believe the severity of this toxicity is attributable to the mouse background, as NOD/SCID mice harbor the mutated *Prkdc* gene which makes them much more sensitive to radiation than athymic mice or humans (37, 38). We too observed dose-dependent hematologic toxicity in our studies, but overt and concerning toxicity (i.e., petechiae) was only observed in a minority of Lu-149 bearing mice in the cohort receiving the highest activity dose of [$^{177}$Lu]Lu-DTPA-CHX-A"-SC16, while none of the H82-bearing mice demonstrated severe petechiae. The blood components also recovered back to pretreatment levels, suggesting that the toxicity does not have long-term implications.

In conclusion, the remarkable efficacy, durability of tumor responses, and low toxicity of [$^{177}$Lu]Lu-DTPA-CHX-A"-SC16 treatment indicates that this is a promising candidate for clinical translation in the treatment of SCLC. While the present work focuses on targeting DLL3 using radioimmunotherapy for SCLC, DLL3 is expressed at comparable levels on the cell surface of other tumor types including neuroendocrine prostate cancer and glioma, implying that this therapeutic approach could be widely applicable for malignancies with aberrant DLL3 expression (30, 39).

## Authors' Disclosures

K.M. Tully reports grants from Weill Cornell Graduate School of Medical Sciences (New York, NY) during the conduct of the study; in addition, K.M. Tully has a patent for Dll3-targeting antibodies and uses thereof pending. J.A. Korsen reports grants from Weill Cornell Medicine during the conduct of the study. J.T. Poirier reports grants from NCI during the conduct of the study; in addition, J.T. Poirier has a patent for Dll3-targeting antibodies and uses thereof pending. C.M. Rudin reports personal fees from AbbVie, Amgen, AstraZeneca, Epizyme, Genentech/Roche, Ipsen, Jazz, Eli Lilly and Company, Syros, Bridge Medicines, Harpoon Therapeutics, and Earli outside the submitted work; in addition, C.M. Rudin has patents for PCT/US2020/041282, 63/240,216, and 63/240,237 pending. J.S. Lewis reports grants from NIH and Tri-Institutional Therapeutics Discovery Institute (New York, NY) during the conduct of the study; in addition, J.S. Lewis has a patent for WO2021007371A1 pending. No disclosures were reported by the other authors.

## Authors' Contributions

**K.M. Tully:** Conceptualization, formal analysis, investigation, visualization, methodology, writing–original draft, project administration, writing–review and editing. **S. Tendler:** Formal analysis, investigation, methodology, writing–review and editing. **L.M. Carter:** Data curation, software, formal analysis, investigation, methodology, writing–original draft, writing–review and editing. **S.K. Sharma:** Conceptualization, supervision, funding acquisition, investigation, methodology, writing–review and editing. **Z.V. Samuels:** Investigation, methodology, writing–review and editing. **K. Mandleywala:** Investigation, methodology, writing–review and editing. **J.A. Korsen:** Formal analysis, validation, investigation, visualization, methodology, writing–review and editing. **A.M. Delos Reyes:** Investigation, methodology, writing–review and editing. **A. Piersigilli:** Validation, investigation, methodology, writing–original draft. **W.D. Travis:** Validation, investigation, methodology, writing–review and editing. **T. Sen:** Supervision, writing–review and editing. **N. Pillarsetty:** Conceptualization, formal analysis, supervision, visualization, writing–original draft, writing–review and editing. **J.T. Poirier:** Conceptualization, resources, supervision, funding acquisition, visualization, methodology, writing–original draft, writing–review and editing. **C.M. Rudin:** Conceptualization, resources, supervision, funding acquisition, visualization, methodology, writing–original draft, writing–review and editing. **J.S. Lewis:** Conceptualization, resources, supervision, funding acquisition, visualization, methodology, writing–original draft, writing–review and editing.

## Acknowledgments

This work was supported in part by NIH grants U01 CA213359 and R01 CA213448 (to J.T. Poirier, C.M. Rudin, J.S. Lewis), R35 CA263816 (to C.M. Rudin), and R35 CA232130 (to J.S. Lewis). K.M. Tully was supported by the Weill Cornell Graduate School of Medical Sciences (grant no. T32 GM073546) Predoctoral Training Grant in Pharmacological Sciences. Technical services provided by the Memorial Sloan Kettering Cancer Center Small-Animal Imaging Core Facility, supported in part by NIH Cancer Center Support Grant P30 CA008748, are gratefully acknowledged. NIH Shared Instrumentation Grant S10 RR028889, which provided funding support for the purchase of the NanoSPECT/CT Plus, is gratefully acknowledged. Finally, the authors gratefully acknowledge the Memorial Sloan Kettering Cancer Center Anti-Tumor Assessment Core, the Memorial Sloan Kettering Molecular Cytology Core, and the Tri-Institutional Laboratory of Comparative Pathology.

The costs of publication of this article were defrayed in part by the payment of page charges. This article must therefore be hereby marked *advertisement* in accordance with 18 U.S.C. Section 1734 solely to indicate this fact.

Received April 26, 2021; revised October 18, 2021; accepted January 13, 2022; published first January 18, 2022.

## References

1. Gazdar AF, Bunn PA, Minna JD. Small-cell lung cancer: what we know, what we need to know and the path forward. Nat Rev Cancer 2017;17:725–37.
2. Sabari JK, Lok BH, Laird JH, Poirier JT, Rudin CM. Unravelling the biology of SCLC: implications for therapy. Nat Rev Clin Oncol 2017;14:549–61.
3. Oronsky B, Reid TR, Oronsky A, Carter CA. What's new in SCLC? A review. Neoplasia 2017;19:842–7.
4. Rudin CM, Brambilla E, Faivre-Finn C, Sage J. Small-cell lung cancer. Nat Rev Dis Primers 2021;7:3.
5. Dowell JE. Small cell lung cancer: are we making progress? Am J Med Sci 2010;339:68–76.
6. Saunders LR, Bankovich AJ, Anderson WC, Aujay MA, Bheddah S, Black K, et al. A DLL3-targeted antibody-drug conjugate eradicates high-grade pulmonary neuroendocrine tumor-initiating cells in vivo. Sci Transl Med 2015;7:302ra136.
7. Borromeo MD, Savage TK, Kollipara RK, He M, Augustyn A, Osborne JK, et al. ASCL1 and NEUROD1 reveal heterogeneity in pulmonary neuroendocrine tumors and regulate distinct genetic programs. Cell Rep 2016;16:1259–72.
8. Furuta M, Kikuchi H, Shoji T, Takashima Y, Kikuchi E, Kikuchi J, et al. DLL3 regulates the migration and invasion of small cell lung cancer by modulating Snail. Cancer Sci 2019;110:1599–608.
9. Yan LX, Liu YH, Li Z, Luo DL, Li YF, Yan JH, et al. Prognostic value of delta-like protein 3 combined with thyroid transcription factor-1 in small-cell lung cancer. Oncol Lett 2019;18:2254–61.

10. Rudin CM, Poirier JT, Byers LA, Dive C, Dowlati A, George J, et al. Molecular subtypes of small cell lung cancer: a synthesis of human and mouse model data. Nat Rev Cancer 2019;19:289–97.
11. Chapman G, Sparrow DB, Kremmer E, Dunwoodie SL. Notch inhibition by the ligand DELTA-LIKE 3 defines the mechanism of abnormal vertebral segmentation in spondylocostal dysostosis. Hum Mol Genet 2011;20:905–16.
12. Geffers I, Serth K, Chapman G, Jaekel R, Schuster-Gossler K, Cordes R, et al. Divergent functions and distinct localization of the Notch ligands DLL1 and DLL3 in vivo. J Cell Biol 2007;178:465–76.
13. Huang RSP, Holmes BF, Powell C, Marati RV, Tyree D, Admire B, et al. Delta-like protein 3 prevalence in small cell lung cancer and DLL3 (SP347) assay characteristics. Arch Pathol Lab Med 2019;143:1373–7.
14. Tanaka K, Isse K, Fujihira T, Takenoyama M, Saunders L, Bheddah S, et al. Prevalence of Delta-like protein 3 expression in patients with small cell lung cancer. Lung Cancer 2018;115:116–20.
15. Rojo F, Corassa M, Mavroudis D, Oz AB, Biesma B, Brcic L, et al. International real-world study of DLL3 expression in patients with small cell lung cancer. Lung Cancer 2020;147:237–43.
16. Owen DH, Giffin MJ, Bailis JM, Smit MD, Carbone DP, He K. DLL3: an emerging target in small cell lung cancer. J Hematol Oncol 2019;12:61.
17. Johnson ML, Zvirbule Z, Laktionov K, Helland A, Cho BC, Gutierrez V, et al. Rovalpituzumab tesirine as a maintenance therapy after first-line platinum-based chemotherapy in patients with extensive-stage-SCLC: results from the phase 3 MERU study. J Thorac Oncol 2021;16:1570–81.
18. Blackhall F, Jao K, Greillier L, Cho BC, Penkov K, Reguart N, et al. Efficacy and safety of rovalpituzumab tesirine compared with topotecan as second-line therapy in DLL3-high SCLC: results from the phase 3 TAHOE study. J Thorac Oncol 2021;16:1547–58.
19. Taveras C, editor. AbbVie discontinues rovalpituzumab tesirine (Rova-T) research and development program. Illinois: AbbVie Inc.; 2019.
20. Morgensztern D, Besse B, Greillier L, Santana-Davila R, Ready N, Hann CL, et al. Efficacy and safety of rovalpituzumab tesirine in third-line and beyond patients with DLL3-expressing, relapsed/refractory small-cell lung cancer: results from the phase II TRINITY study. Clin Cancer Res 2019;25:6958–66.
21. Poirier JT, George J, Owonikoko TK, Berns A, Brambilla E, Byers LA, et al. New approaches to SCLC therapy: from the laboratory to the clinic. J Thorac Oncol 2020;15:520–40.
22. Takada M, Fukuoka M, Kawahara M, Sugiura T, Yokoyama A, Yokota S, et al. Phase III study of concurrent versus sequential thoracic radiotherapy in combination with cisplatin and etoposide for limited-stage small-cell lung cancer: results of the Japan clinical oncology group study 9104. J Clin Oncol 2002;20:3054–60.
23. Slotman B, Faivre-Finn C, Kramer G, Rankin E, Snee M, Hatton M, et al. Prophylactic cranial irradiation in extensive small-cell lung cancer. N Engl J Med 2007;357:664–72.
24. Auperin A, Arriagada R, Pignon JP, Le Pechoux C, Gregor A, Stephens RJ, et al. Prophylactic cranial irradiation for patients with small-cell lung cancer in complete remission. Prophylactic cranial irradiation overview collaborative group. N Engl J Med 1999;341:476–84.
25. Sharma SK, Pourat J, Abdel-Atti D, Carlin SD, Piersigilli A, Bankovich AJ, et al. Noninvasive interrogation of DLL3 expression in metastatic small cell lung cancer. Cancer Res 2017;77:3931–41.
26. Hindie E, Zanotti-Fregonara P, Quinto MA, Morgat C, Champion C. Dose deposits from 90Y, 177Lu, 111In, and 161Tb in micrometastases of various sizes: implications for radiopharmaceutical therapy. J Nucl Med 2016;57:759–64.
27. O'Donoghue JA, Bardies M, Wheldon TE. Relationships between tumor size and curability for uniformly targeted therapy with beta-emitting radionuclides. J Nucl Med 1995;36:1902–9.
28. Phelps RM, Johnson BE, Ihde DC, Gazdar AF, Carbone DP, McClintock PR, et al. NCI-navy medical oncology branch cell line data base. J Cell Biochem Suppl 1996;24:32–91.
29. Laird JH, Lok BH, Ma J, Bell A, de Stanchina E, Poirier JT, et al. Talazoparib is a potent radiosensitizer in small cell lung cancer cell lines and xenografts. Clin Cancer Res 2018;24:5143–52.
30. Puca L, Gavyert K, Sailer V, Conteduca V, Dardenne E, Sigouros M, et al. Delta-like protein 3 expression and therapeutic targeting in neuroendocrine prostate cancer. Sci Transl Med 2019;11:eaav0891.
31. Sano R, Krytska K, Tsang M, Erickson SW, Teicher BA, Saunders L, et al. Abstract LB-136: pediatric preclinical testing consortium evaluation of a DLL3-targeted antibody drug conjugate rovalpituzumab tesirine, in neuroblastoma. Cancer Res 2018;78:LB–136.
32. Harada T, Maronpot RR, Enomoto A, Tamano S, Ward JM. Changes in the liver and gallbladder. In: Mohr U, Dungworth DL, Capen CC, Carlton WW, Sundberg JP, Ward JM, editors. Washington, DC: ILSI Press; 1996. p. 207–41.
33. Thoolen B, Maronpot RR, Harada T, Nyska A, Rousseaux C, Nolte T, et al. Proliferative and nonproliferative lesions of the rat and mouse hepatobiliary system. Toxicol Pathol 2010;38:5S–81S.
34. Faccini J, Abbott DP, Paulus G. Mouse Histopathology: A glossary for use in toxicity and carcinogenicity studies. Amsterdam (Netherlands): Elsevier; 1990.
35. US Congress. H.R.733 — Recalcitrant Cancer Research Act of 2012, 112th Cong., 1st Sess. (2012).
36. Lakes AL, An DD, Gauny SS, Ansoborlo C, Liang BH, Rees JA, et al. Evaluating (225)Ac and (177)Lu radioimmunoconjugates against antibody-drug conjugates for small-cell lung cancer. Mol Pharm 2020;17:4270–9.
37. Fulop GM, Phillips RA. The scid mutation in mice causes a general defect in DNA repair. Nature 1990;347:479–82.
38. Biedermann KA, Sun JR, Giaccia AJ, Tosto LM, Brown JM. scid mutation in mice confers hypersensitivity to ionizing radiation and a deficiency in DNA double-strand break repair. Proc Natl Acad Sci U S A 1991;88:1394–7.
39. Spino M, Kurz SC, Chiriboga L, Serrano J, Zeck B, Sen N, et al. Cell surface notch ligand DLL3 is a therapeutic target in isocitrate dehydrogenase-mutant glioma. Clin Cancer Res 2019;25:1261–71.